RECTANGULAR MORTISE AND FULL-WIDTH TENON JOINTS IN READY-TO-ASSEMBLE LIGHT-FRAME TIMBER CONSTRUCTIONS

Carl A. Eckelman†

Professor
E-mail: eckelmac@purdue.edu

*Eva Haviarova**†

Associate Professor
Department of Forestry and Natural Resources
Purdue University
West Lafayette, IN
E-mail: ehaviar@purdue.edu

(Received March 2011)

Abstract. Research has demonstrated the suitability of light-frame timber constructions for ready-to-assemble housing. In this study, tests were conducted to determine the semirigid rotation characteristics of full-width mortise and tenon joints along with their moment capacity. Semirigid rotation factors varied from 12.27×10^{-6} rad/N·m for joints with 37.9-mm-thick × 146.1-mm-deep rails with 93.0-mm-deep tenons to 2.57×10^{-6} rad/N·m for 36.5-mm-thick × 254.0-mm-deep rails with 200.2-mm-deep tenons. Moment capacity of joints with full-width tenons varied from 9360 N·m for 36.5-mm-thick × 254-mm-deep rails with 200.2-mm-deep tenons to 2810 N·m for joints with 37.9-mm-thick × 146.1-mm-deep rails with 93.0-mm-deep tenons. Moment capacity of the joints could be closely estimated by regression expressions that take into account shear area along the neutral axis between the cross-pin and the end of the tenon and shear area of the relish itself.

Keywords: Rectangular mortise and tenon joints, full-width tenons, ready-to-assemble light-frame timber constructions.

INTRODUCTION

Light-frame timber constructions that incorporate ready-to-assemble concepts have several potential uses, especially in construction of frames for transitional disaster relief housing. "Built-up" mortise and tenon joints with full-width tenons (ie without shoulders) similar to that shown in Fig 1 appear to be well suited for construction of ready-to-assemble frames mostly because of simple assembly without the need for specialized tools. Ends of members such as studs are simply inserted into mortises in mating members such as sills and wall plates and are pinned in place. Mortise and tenon joints are also of particular interest because they have a long history of use in house, barn, and bridge construction and are known and accepted in many areas of the world. Similarly, "built-up" sills and plates along with posts have a long history of use; built-up sills, for example, are described in early textbooks of the 1900s (Townsend 1907) and built-up girders are described by Anderson and Heyer (1955). Finally, preferred vertically laminated beam practices are well documented (USDA 1940, 1955) as is nail gluing (Radcliffe and Granum 1954; Karlsen 1967) and horizontally nail-laminated beams (Bohnhoff 1992).

Key elements of a built-up mortise and tenon ready-to-assemble system are mortised sills, plates, or posts that are built-up (eg nail-glued) from standard members into which studs, joists, or other members may be inserted (Fig 1). In the field, a skeleton structure such as that shown in Fig 2a might be rapidly erected and covered with canvas and subsequently, studs and rafters added along with horizontal nailers. The resultant frame may be roofed and sided in a manner similar to that shown in Fig 2b.

* Corresponding author
† SWST member

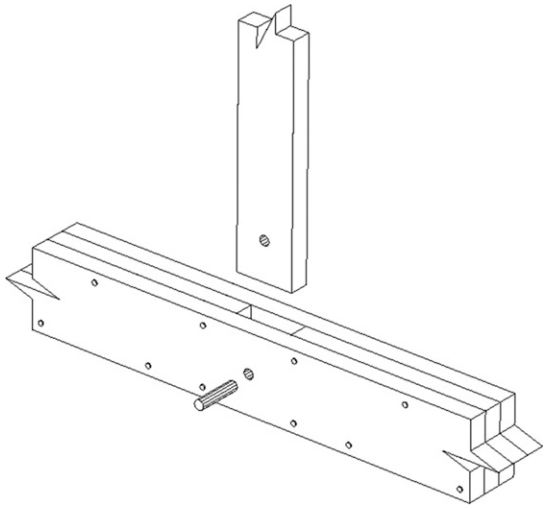

Figure 1. Built-up nail-glued mortise and tenon joint construction.

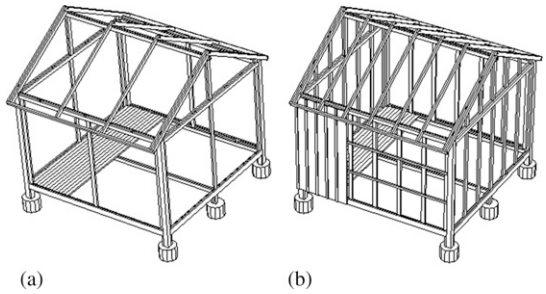

Figure 2. (a) Initial transitional skeleton tent frame constructed with built-up mortise and tenon joints; (b) drawing of structure after additional rafters, studs, and horizontal nailers have been added and partial vertical siding applied.

Rational analysis and design of such constructions require information concerning stiffness characteristics of the joints. In service, these frames will be subjected to substantial wind loads, and information concerning joint stiffness is needed to ensure that internal resisting forces are, to the extent possible, evenly distributed throughout the frame. Also, in a simple corner support foundation system, side walls act as Vierendeel trusses, and their analyses require joint stiffness information.

Other applications of ready-to-assemble light-frame designs include the construction of bents,

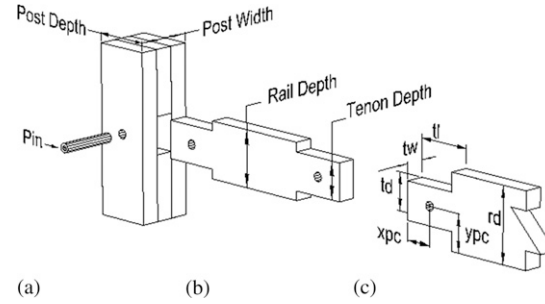

Figure 3. Configuration of typical specimen showing (a) post, (b) rail, and (c) tenon nomenclature.

eg in which floor sills and ceiling joists frame into mortises in built-up posts. Rational design of these frames also dictates that information be available concerning the semirigid rotation characteristics of joints.

To obtain rational estimates of stiffness characteristics of such joints, a limited study was undertaken (as part of an ongoing study dealing with light-frame timber construction). Also collected was information concerning semirigid rotation characteristics of representative mortise and tenon joints with full-width tenons and incidental information concerning their moment capacity. A brief follow-up study also was conducted to evaluate factors controlling moment capacity of partial-width tenons.

MATERIAL AND METHODS

Specimen Preparation

A complete specimen consisted of a rail with a tenon machined on each end (Fig 3b) and a corresponding post (Fig 3a) that contained a matching mortise. Symbolic definitions of specimen dimensions are given in Fig 3c. All rails were constructed of nominal 38-mm-thick locally obtained yellow-poplar (*Liriodendron tulipifera*) that had been conditioned to 7% MC. Yellow-poplar was selected because it was thought that its properties would be similar to those of low-strength hardwoods growing in tropical disaster areas. Posts were of laminated three-ply construction (assembled with polyvinyl adhesive) and were constructed from

the same pool of nominal 38-mm-thick material used for the rails. Thus, width (Fig 3a) of each post was triple the width of the rails, whereas depth (Fig 3b) of each post was equal to length of the corresponding tenon. The center laminate of each post (Fig 3a) consisted of two pieces that were spaced an appropriate distance apart longitudinally to create a mortise depth equal to the corresponding tenon depth. Post length was a nominal 457 mm. Rail length varied from a nominal 530-760 mm and was increased in proportion to rail depth. Dimensions of rails and tenons are given in Table 1. Pin diameters and locations are also given in Table 1. Most cross-pins were constructed of standard black pipe with 21.5-mm diameter; however, seven were constructed with 25.4-mm steel dowels and four with 33.4-mm steel dowels (Table 1).

Dimensions of the partial-width specimens are given in Table 2. Nominal width of the rails and posts was 112 mm, whereas nominal width of the tenons was 37 mm. These members were laminated from the same pool of material used in the previous specimens, but shortage of material dictated the use of somewhat smaller rail depths.

Test Methods

Specimens were supported for testing in a manner similar to that shown in Fig 4. Rate of loading was 6.0 mm/min. Moment arm, *L*, varied from 305-508 mm. Rotations of the rails relative to the posts were determined by means of two dial gages spaced 254 mm apart (dimension [g], Fig 4). Deflection readings of the dial gages were recorded at regular load intervals and load vs deflection data saved in a spreadsheet. Procedurally, when the second tenon on a rail was tested, the mortised member was rotated 180 deg about the longitudinal axis of

Table 1. Bending moment capacity and semirigid rotation coefficients for full-width tenons[a]

Specimen	Pin diam. (mm)	Rail depth *rd* (mm)	Tenon depth *td* (mm)	Tenon width *tw* (mm)	Tenon length *tl* (mm)	Bottom edge to pin center *ypc* (mm)	Tenon end to pin center *xpc* (mm)	Ultimate moment capacity (N·m)	Semirigid rotation factor (10^{-6}) rad/N·m
4	21.5	137.7	93.0	37.9	152.4	68.8	76.2	2,770	na[b]
4	21.5	137.7	93.0	37.9	152.4	68.8	38.1	2,890	na
4	21.5	137.7	93.0	37.9	152.4	68.8	114.3	3,220	na
4	21.5	254.0	200.2	36.5	254.0	184.2	63.5	9,360	2.57
7	25.4	254.0	200.2	36.5	254.0	127.0	127.0	9,330	4.71
3	21.5	203.2	149.4	36.5	145.9	101.6	74.7	4,220	7.79
2	21.5	203.2	149.4	36.5	145.9	139.7	41.4	3,490	5.84
4	33.4	203.2	149.4	35.1	145.9	101.6	71.4	3,950	10.58
4	33.4	177.8	93.0	35.1	145.9	88.9	66.8	2,520	12.66
3	21.5	171.5	119.4	37.9	152.4	85.9	76.2	3,920	8.31
3	21.5	146.1	93.0	37.9	152.4	73.2	73.2	3,540	9.27
3	21.5	146.1	93.0	37.9	152.4	73.2	44.5	2,810	12.27

[a] Joint dimension notation given in Fig 3.
[b] Joint rotation was not measured.

Table 2. Bending moment capacity of joints with partial-width tenons[a]

Specimen	Rail width (mm)	Rail depth *rd* (mm)	Tenon depth *td* (mm)	Tenon width *tw* (mm)	Tenon length *tl* (mm)	Bottom edge to pin center *ypc* (mm)	Tenon end to pin center *xpc* (mm)	Moment capacity (N·m)
2	116.6	95.3	69.9	38.4	108.0	47.6	54.0	2713
3	111.9	146.7	69.9	35.5	147.6	73.6	73.8	3150
2	111.9	146.7	92.6	37.0	147.6	73.6	73.8	4886
4	111.9	146.7	118.8	37.0	147.6	73.6	73.8	6217
4	111.9	146.7	149.1	37.0	147.6	73.6	73.8	4812
4	111.9	197.5	198.5	37.0	197.5	98.8	98.8	8554
4	111.9	250.8	198.5	37.0	254.0	125.4	127.0	13,997

[a] Joint dimension notation given in Fig 3.

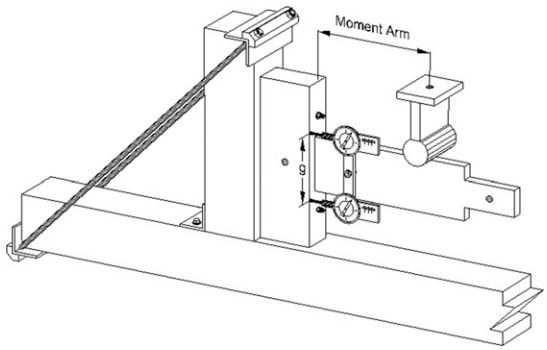

Figure 4. Apparatus used to determine moment rotation characteristics and moment capacity of specimens.

the mortise to provide a new bearing surface for the shoulder of the tenon inserted into it.

Data Analysis

Combined absolute values of gauge displacements at each recorded moment level were divided by distance between gauges, and resulting rotations were plotted as a function of moment for each specimen. Deflection of the rail itself was assumed to be negligible. A regression expression of the form $\varphi = a + bM$ was then fitted to the lower, ie linear, portion of the curve, where φ refers to semirigid joint rotation, a and b are regression coefficients, and M refers to bending moment acting on the joint. Semirigid joint connection factors (Lothers 1960), Z, were then taken as the slope of the regression expression, ie $Z = b$.

RESULTS AND DISCUSSION

Semirigid Joint Factors

Semirigid connection factors for various joint constructions are given in Table 1 and are shown in Fig 5. Accompanying joint nomenclature is given in Fig 3. As can be seen in Fig 5, rotations were relatively well associated with joint geometry and varied from a minimum of 2.57×10^{-6} rad/N·m for 254.0-mm-deep (*rd*, Fig 3) rails to a maximum of 12.27×10^{-6} rad/N·m for 146.1-mm-deep rails.

Comparison of rotation of the 177.8-mm-deep rails, 12.66×10^{-6} rad/N·m, with the slightly

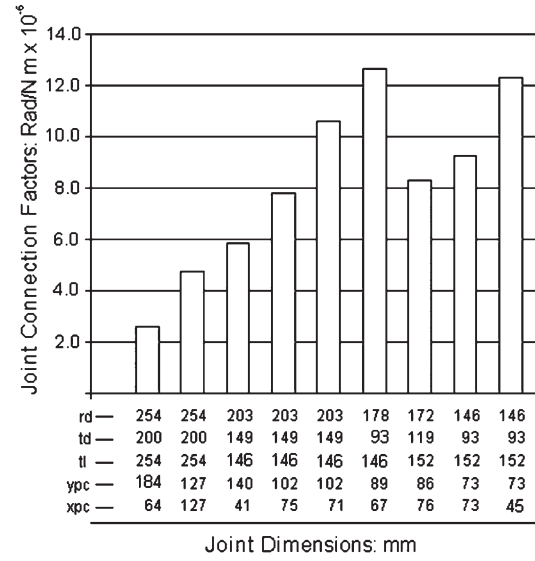

Figure 5. Semirigid joint connection factors (rd = rail depth; td = tenon depth; tl = tenon length; ypc = distance from rail edge to pin center; xpc = distance from end of tenon to pin center).

smaller specimens with 171.5-mm-deep rails, 8.31×10^{-6} rad/N·m, indicated that specimens were sensitive to tenon depth (*td*, Fig 3), ie 93.0 vs 119.4 mm. Also, difference in rotations of the 146.1-mm-deep specimens (9.27×10^{-6} vs 12.27×10^{-6} rad/N·m) appeared to be a function of cross-pin placement (*xpc*, Fig 3) along the length of the tenon.

Inspection of residual permanent deformations of specimens after testing indicated that semirigid joint rotation resulted primarily from compression of wood on the bottom side of the tenon at its point of entry into the mortise (point *a*, Fig 6), compression of the top side of the tenon at its point of exit from the mortise (point *b,* Fig 6), the compression of wall of the mortise by the bottom shoulder of the tenon (point *c*, Fig 6), and compression of the mortise walls beneath the ends of the cross-pins (point *d*, Fig 6). Of these, crushing of the mortise wall by the bottom shoulder of the tenon (point *c*, Fig 6) appeared to be a major contributor to semirigid rotation and is related to side hardness (Eckelman et al 2008) of wood. Thus,

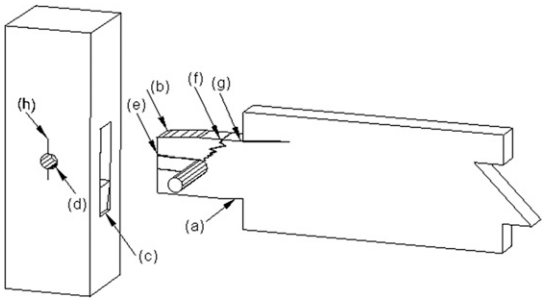

Figure 6. Points of deformation or failure of specimens.

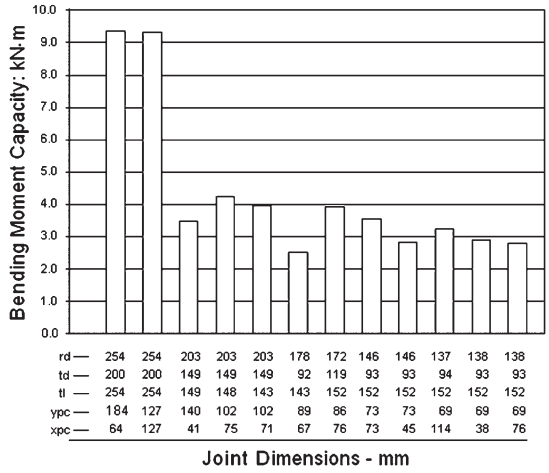

Figure 7. Bending moment capacities of full-width tenons (rd = rail depth; td = tenon depth; tl = tenon length; ypc = distance from rail edge to pin center; xpc = distance from end of tenon to pin center).

joints constructed of red oak (side hardness: 5.7 kN; FPL 1999) would be expected to have a lower rotation factor than those constructed of yellow-poplar (side hardness: 2.4 kN). This relationship was previously noted in a study of round mortise and tenon joints (Eckelman et al 2008).

Moment Capacity

Results of moment capacity tests for full-width tenons are given in Table 1 and are shown in Fig 7. Results for partial-width tenons are given in Table 2.

Expected mode of failure of pinned mortise and tenon joints attributed to moment was either single or double shear of the relish (point *e*, Fig 6). As pointed out by Miller (2004), a single shear failure is load limiting but the joint continues to hold the failing load, whereas a double shear failure results in loss of load. However, other types of failure may also occur, such as perpendicular-to-grain failure of the mortise wall (point *h*, Fig 6). In this respect, in tension tests conducted with 19.05-mm red oak pegs, Schmidt and MacKay (1997) indicated that to prevent the sides of the mortise from splitting, distance from the center of the peg to the edge of the mortise should be at least four times the peg diameter.

Additional types of failure include bending fracture of tenon at root of tenon (point f, Fig 6), perpendicular-to-grain failure of tenon shoulder at the root of the tenon (point *g*, Fig 6), and crushing of the mortise wall beneath the cross-pin (point *d*, Fig 6). For joints of the configuration used in this study, however, single or double shear of the relish as a function of the force exerted by the cross-pin and shear force acting along the neutral axis of the tenon was the expected mode of failure. It was assumed, therefore, that a regression expression used to describe the test results should take into account shear area of the relish and shear area along the neutral axis of the tenon. Thus, a regression expression of the form

$$M = a_1 \times \left[a_2 \times \left(tw^2 \times td \times (tl - pd)\right) + a_3 \times (2 \times tw \times xpc) \times ypc\right] \quad (1)$$

was used to relate moment capacity to joint geometry where M refers to moment, pd to pin diameter, tw to tenon width, td to tenon depth, tl to tenon length, xpc to distance from the end of the tenon to pin center, ypc to distance from the bottom edge of the rail to pin center, and a_1, a_2, and a_3 are regression coefficients.

When Eq 1 was fitted to the data (with a_3 set equal to 1.0), the following resulted:

$$M = 215.7 \times \left[2.14 \times \left(tw^2 \times td \times (tl - pd)\right) + (2 \times tw \times xpc) \times ypc\right] \quad (2)$$

with a coefficient of multiple determination of 95.45%. An evaluation of the difference between moment capacities estimated by Eq 2 and test values, ie

$$\text{Dif}(\%) = 100x\,(\text{test} - \text{estimated})/\text{test}$$

gave maximum and minimum deviations of 26.7% and –18.5%, respectively, with a standard deviation of 11.1%.

An evaluation of moment capacities estimated by Eq 2 indicated that the neutral axis shear capacity term, ie

$$215.7 \times \left(2.14 \times tw^2 \times td \times (tl - pd)\right) \quad (3)$$

accounted for 79.3% of the moment capacity whereas the relish shear capacity term, ie

$$215.7 \times (2 \times tw \times xpc \times ypc) \quad (4)$$

accounted for 20.7%. A possible explanation for this outcome is that crushing of the mortise wall by the bottom tenon shoulder (point *c*, Fig 6) limited development of relish shear stress.

In this respect, if a new regression analysis is carried out using only the left side (3) of the equation, ie

$$M = a_1 \times \left[2.14 \times tw^2 \times td \times (tl - pd)\right] \quad (5)$$

the following equation results:

$$M = 265.1 \times \left[2.14 \times tw^2 \times td \times (tl - pd)\right] \quad (6)$$

with coefficient of multiple determination of 94.45% and maximum and minimum deviations (as previously defined) of 31.4% and –18.9%, respectively, and a standard deviation of 12.7%. This result indicates that moment capacity of joints can be estimated almost as well by the neutral axis portion of the equation alone as by the total equation.

In contrast, if only the right side of Eq 4 is considered, ie

$$M = a_1 \times [2 \times tw \times xpc \times ypc] \quad (7)$$

the following equation is obtained:

$$M = 1097.6 \times [2 \times tw \times xpc \times ypc] \quad (8)$$

with coefficient of multiple determination of 77.66% and maximum and minimum deviations of 53.6% and –57.1%, respectively, and a standard deviation of 27.2%.

Elements of the complete equation (namely, *tl* and *td*) are embedded in both the left and right sides of the equation, therefore these results are not entirely independent. However, the proportion of variance explained by the left side of the equation tends to support the conclusion that moment capacity in joints with full-width tenons is determined mostly by the shear area along the neutral axis and the accompanying depth of the tenon.

Partial-Width Tenons

When Eq 1 for full-width tenons is fitted to moment capacity data for partial-width tenons, the following equation results:

$$M = 1321.6 \times \left[0.142 \times tw^2 \times td \times (tl - pd) + (2 \times tw \times xpc) \times ypc\right] \quad (9)$$

with coefficient of multiple determination of 94.72% and maximum and minimum deviations of 31.89% and –35.38%, respectively, and standard deviation of 19.0%. In this equation, the left side (neutral axis shear plane) accounts for only 22.9% of estimated moment capacity, whereas the right side (relish shear planes) accounts for 76.7%.

This result indicates that longitudinal shear along the neutral axis has decidedly less effect on the moment capacity of these specimens than on the moment capacity of full-width specimens. If a regression analysis is carried out using only the relish (right) side of Eq 9, ie

$$M = a_1 \times (2 \times tw \times (tl/2) \times ypc)$$

the following equation results:

$$M = 1726.2 \times (2 \times tw \times (tl/2) \times ypc) \quad (10)$$

with coefficient of multiple determination of 94.02% and maximum and minimum deviations of 30.83% and –52.17%, respectively, and a standard deviation of 23.6%.

This result again indicates that moment capacity of partial-width tenons was dependent largely on shear area of the relish and distance from the edge of the rail to the cross-pin center.

CONCLUSIONS

Semirigid rotation of full-width mortise and tenon joints was directly related to the geometry of the joints. Rotation factors varied from 12.27×10^{-6} rad/N·m for joints with 146.1-mm-deep rails and 93.0-mm-deep tenons to 2.57×10^{-6} rad/N·m for 254.0-mm-deep rails with 200.2-mm-deep tenons when tenon length was nominally equal to rail depth. Semirigid rotation results from (a) compression of wood on the bottom side of the tenon at its point of entry into the mortise, (b) compression of the top side of the tenon at its point of exit from the mortise (at its tip), (c) compression of the wall of the mortise by the bottom shoulder of the tenon, and (d) compression of mortise walls beneath ends of cross-pins.

Moment capacity of mortise and tenon joints can be estimated by equations that take into account shear area along the neutral axis between the cross-pin and the end of the tenon and shear area of the relish. In the case of full-width tenons, ultimate moment capacity was found to be largely dependent on neutral axis shear area. In contrast, moment capacity of partial-width tenons was found to be largely dependent on relish area and distance from the edge of the rail to the center of the cross-pin.

REFERENCES

Anderson LO, Heyer OC (1955) Wood-frame house construction. Ag. Handb 73. US Department of Agriculture, Washington, DC. 235 pp.

Bohnhoff DR (1992) Modeling horizontally nail-laminated beams. J Struct Eng 118(5):1393-1406.

Eckelman AC, Haviarova E, Akcay H (2008) Exploratory study of the moment capacity and semi-rigid moment-rotation behavior of round mortise and tenon joints. Forest Prod J 58(7/8):56-61.

FPL (1999) Wood handbook: Wood as an engineering material. Gen Tech Rep FPL-GTR-113 USDA For Serv Forest Prod Lab, Madison, WI. 463 pp.

Karlsen GG (1967) Wooden structures. MIR Publishers, Moscow. 638 pp.

Lothers JE (1960) Advanced design in structural steel. Prentice-Hall, Englewood Cliffs, NJ. 583 pp.

Miller JF (2004) Capacity of pegged mortise and tenon joinery. MS thesis. University of Wyoming, Laramie, WY. 77 pp.

Radcliffe BM, Granum H (1954) Design of nail-glued plywood gusset plates and solid-wood splice plates for softwoods. Station Bull 613, Agric Exp Stn, Purdue University, West Lafayette, IN.

Schmidt RJ, MacKay RB (1997) Timber frame tension joinery. University of Wyoming, Laramie, WY. 87 pp.

Townsend G (1907) Carpentry and joinery. Technical World Magazine. Chicago. 145 pp.

USDA (1940) Wood handbook. US Department of Agriculture, Washington, DC. 325 pp.

USDA (1955) Wood handbook. Ag Handb 72. US Department of Agriculture, Washington, DC. 528 pp.